Measurement and modelling of the near-field structure of large-scale sonic CO2 releases from pipelines

Robert M. Woolley, Michael Fairweather, Christopher J. Wareing, Samuel A.E.G. Falle, Christophe Proust, Jérôme Hebrard, Didier Jamois

Measurement and Modelling of the Near-field Structure of Large-scale Sonic CO_2 Releases from Pipelines

Robert M. Woolley,[a]* Michael Fairweather,[a] Christopher J. Wareing,[a] Samuel A.E.G. Falle,[b] Christophe Proust,[c] Jerome Hebrard,[c] Didier Jamois[c]

[a] *School of Process, Environmental and Materials Engineering, University of Leeds, Leeds LS2 9JT, UK.*
[b] *School of Mathematics, University of Leeds, Leeds LS2 9JT, UK.*
[c] *INERIS, Dept. PHDS, Parc Technologique ALATA, BP 2, 60550 Verneuil-en-Halatte, France*
**r.m.woolley@leeds.ac.uk*

Abstract

The work presented in this paper describes a novel multi-phase discharge and dispersion model capable of predicting the near-field fluid dynamics and phase-transition phenomena associated with accidental CO_2 releases. Also presented in this paper are previously unpublished data describing the near-field structure of a number of large-scale CO_2 experimental releases, obtained through the EU-FP7 CO2PipeHaz (2009) project. The calculations employed an adaptive finite-volume grid algorithm to solve the Favre-averaged fluid-flow equations. This equation set was closed with the inclusion of both a two-equation k-ε model and a second-moment Reynolds stress model to represent turbulent fluctuations. Results demonstrate the superior performance of the Reynolds stress transport model when compared to its compressibility-corrected counterpart.

Keywords: CO_2; high pressure pipeline; CFD modelling; second-moment closure

1. Introduction

Carbon capture and storage (CCS) refers to a set of technologies which is currently viewed as one of the most promising options for reducing carbon dioxide emissions during the transition period between the current fossil-fuel based economy and that of a new sustainable-energy era. The CCS chain is designed to reduce carbon dioxide emissions from large point-sources of production by extracting CO_2 from flue gases, and its subsequent transportation in dedicated pipelines to facilities such as depleted oil and gas fields or saline aquifers, for the purpose of permanent storage and exclusion from the planet's atmosphere. The transportation network will very likely also involve some means of intermediate storage, and for the design and risk assessment of these components, a quantitative understanding of the consequences of an accidental or operational high-pressure release is required.

The work presented in this paper describes a novel multi-phase discharge and dispersion model capable of predicting the near-field fluid dynamics and phase-transition phenomena associated with accidental CO_2 releases. This represents a significant step towards the development of models capable of accurately predicting the thermofluid behaviour at the interface with the pipe, typically in the vicinity of a crack. These

predictions, including details of heat transfer, can subsequently be used in the formulation of crack propagation and in-pipe behaviour models, thus providing essential information required for pipeline design and regulation. Additionally, the accurate prediction of the correct thermodynamic phase during the discharge process in the near-field is of particular importance given the very different hazard profiles of CO_2 in the gas and solid states. The modelling of CO_2 fluid dynamics therefore poses a unique set of problems, and the theoretical developments presented in this paper go some way to elucidating the observed physics. To date, most modelling techniques have been limited by homogeneous equilibrium assumptions and CO_2 expansion described by one-dimensional calculations. These models can not accurately predict the near-field characteristics of these complex releases which is required in predicting the major hazards used in safety and risk assessments. Also, they cannot be used to assess the impact of such releases on surrounding plant. Previous works concerned with the near-field modelling of CO_2 releases are well covered in a review by Dixon et al. (2012), and Witlox et al. (2013) and Herzog and Egbers (2013) should be consulted for the most recent developments by other research groups. Additionally, the work presented here builds upon previous models, validated against less detailed experimental data sets as described in Woolley et al. (2013). Also presented in this paper are previously unpublished data describing the near-field structure of a number of large-scale CO_2 experimental releases, obtained through the EU-FP7 CO2PipeHaz project (CO2PipeHaz, 2009). These data are used in the validation of the near-field model.

2. Mathematical Modelling

2.1. Turbulent Flow Field

Predictions were based on the solutions of the Favre-averaged, density-weighted forms of the transport equations for mass, momentum, two conserved scalars (CO_2 mass fraction, and CO_2 dense phase fraction), and total energy per unit volume (internal energy plus kinetic energy). This model is capable of representing a fluid flow-field comprising a mixture of CO_2 (vapour/liquid/solid) and air. The equations employed in this study were cast in an axisymmetric form, and further details can be found in Woolley et al. (2013). The equation set is closed via the prescription of the turbulence stress tensor ($\widetilde{u_i''u_j''}$) as prescribed by the k-ε model (Jones and Launder, 1972) and also a second-moment transport model. Although the standard k-ε model has been extensively used for the prediction of incompressible flows, its performance is well known to be poor in the prediction of their compressible counterparts. The model consistently over-predicts turbulence levels and hence mixing due to compressible flows displaying an enhancement of turbulence dissipation. For flows typical of those observed here, a model proposed by Sarkar et al. (1991) has demonstrated the most reliable predictions (Fairweather and Ranson, 2006) when applied. Hence, calculations were undertaken using the modifications to the turbulent Mach number and the turbulence viscosity as prescribed therein. Figure 1 depicts predictions of axial velocity, plotted against the experimental data of a highly under-expanded air jet (Donaldson and Snedeker, 1971), obtained with and without the application of this modification. The intended effect of a notable reduction in the turbulence dissipation is clearly evident. The second-order Reynolds stress model used was that prescribed by Jones and Musonge (1988), modified only in-line with recommendations made by Dianat et al. (1996) for round jets. Eq. (1) represents the transport equation for the turbulence stress tensor in Cartesian tensor notation.

$$\frac{\partial}{\partial t}\left(\bar{\rho}\widetilde{u_i''u_j''}\right)+\frac{\partial}{\partial x_k}\left(\bar{\rho}\widetilde{u_i''u_j''}\tilde{u}_k\right)=C_s\frac{\partial}{\partial x_k}\left(\tau\bar{\rho}\widetilde{u_k''u_l''}\frac{\partial}{\partial x_l}\widetilde{u_k''u_l''}\right)+P_{ij}+A_{ij}-\frac{2}{3}\delta_{ij}\bar{\rho}\varepsilon \quad (1)$$

Figure 1 also depicts predictions of axial velocity, plotted against the experimental data, but obtained using the second-moment turbulence closure. No modification has been made to account for compressibility, and yet its performance can be seen to be in line with that of the corrected k-ε model, and indeed slightly superior.

2.2. Equation of State

The Peng-Robinson equation of state (Peng and Robinson, 1976) is satisfactory for predicting the gas phase properties of CO_2, but when compared to that of Span and Wagner (1996), it is not so for the condensed phase. Furthermore, it is not accurate for gas pressures below the triple point and, in common with any single equation, it does not account for the discontinuity in properties at the triple point. In particular, there is no latent heat of fusion. Span and Wagner (1996) give a formula for the Helmholtz free energy that is valid for both the gas and liquid phases above the triple point, but it does not take account of experimental data below the triple point, nor does it give the properties of the solid. In addition, the formula is too complicated to be used efficiently in a computational fluid dynamics code. A composite equation of state has therefore been constructed to determine the phase equilibrium and transport properties for CO_2. The inviscid version of this model is presented in detail elsewhere (Wareing et al., 2013) and the method reviewed here is now extended for the turbulence closure of the fluid equations detailed in the previous section. In this, the gas phase is computed from the Peng-Robinson equation of state, and the liquid phase and saturation pressure are calculated from tabulated data generated with the Span and Wagner equation of state and the best available source of thermodynamic data for CO_2, the Design Institute for Physical Properties (DIPPR) 801 database, access to which can be gained through the Knovel library (DIPPR, 2013).

2.3. Homogeneous Relaxation Model

A homogeneous relaxation model was developed to represent the relaxation of the condensed phase to equilibrium. In this, the relaxation time was introduced with respect to the transport of the dense phase. A full model requires the inclusion of discrete drops or particles, but it is possible to derive a simple sub-model for the relaxation to equilibrium in which the temperature relaxation is ignored and it is simply assumed that the condensed phase mass fraction is given by its transport equation with an appropriate source term. Again, further details of this model can be found in a previous publication (Woolley et al., 2013)

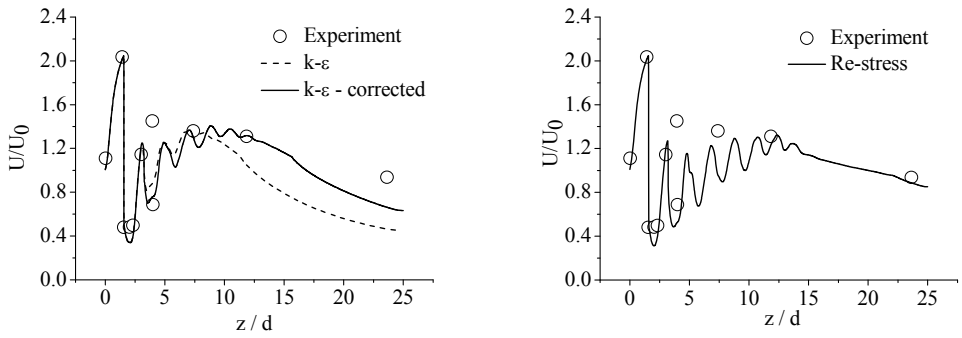

Figure 1: Non-dimensionalised axial velocity predictions in the Donaldson and Snedeker air jet (left – k-ε, right – Reynolds stress).

Figure 2: Experimental rig, including filling sphere and discharge pipe.

The relaxation time chosen to represent behaviour in the near-field of releases such as those considered herein was in the order of 10^{-3} s and obtained by the assessment of the rate that the calculated CO_2 saturation pressure relaxed to the local vapour pressure. In post-shock regions of the flow, a relaxation time of the order 2.5 s was chosen, representing the non-equilibrium state of the condensed phase.

3. Experimental Arrangement

Figure 2 depicts the 2 cubic metre spherical experimental pressure vessel, with the filling sphere in-situ in the foreground, and the discharge pipe exiting the building wall to the right. This spherical pressure vessel is thermally insulated, and can contain up to 1000 kg of CO_2 at a maximum operating pressure and temperature of 200 bar and 473 K, respectively. It is equipped internally with 6 thermocouples and 2 high-precision pressure gauges as well as sapphire observation windows. The vessel has a mass of approximately 5000 kg, and is supported by 4 'Mettler 0745 A' load cells, enabling a continuous measurement of the CO_2 content with an uncertainty of ±500 g. The response time of these devices is fast enough to consider the accurate measurement of mass flow during an experiment, which is obtained by derivation of the best trend-line passing through the points of mass versus time. It is estimated that the accuracy of this technique is ±0.2 $kg.s^{-1}$. The pressure within the sphere is measured using a Piezoresistive-type 'KISTLER 4045 A 200' sensor with a range of 0-200±0.1 bar, and the internal temperature is measured at 6 points on the vertical axis of the sphere using sheathed, 1 mm type-K class-A thermocouples with an accuracy of ± 0.3 °C. The orifices used at the exit plane of the discharge pipe are interchangeable, and are all drilled into a large screwed flange. The thickness of this flange is typically 15 mm and the diameter of the orifice is constant over a length of 10 mm and then expanded with an angle of 45° towards the exterior. Discharge nozzle diameters of 12 and 25 mm, and a full bore of 50 mm were used in these experiments, and further details of the releases are provided in Table 1.

Table 1: Parameters of the experimental releases.

Test Number	Observed Mean Mass Flow Rates / $kg\ s^{-1}$	Ambient Temperature / K	Air Humidity / %	Reservoir Pressure / bar	Nozzle Diameter / mm
11	7.7	276.15	>95	83	12
12	24.0	276.15	>95	77	25
13	40.0	276.65	>95	69	50

4. Results and Discussion

Figure 3 presents calculated centerline temperatures of the three test cases, plotted against the experimental data, and obtained using the Reynolds stress and two-equation turbulence closures. It is evident from these plots that both models qualitatively reproduce the physics present within such releases, and features such as the stationary shock wave are prominent. The effect of the latent heat of fusion can be observed in each of the sets of predictions as a small step-change prior to the shock region. This is indicative of the system passing through the triple point, and the subsequent formation of solids. It can be seen that in all the test cases, little difference is observed between the two closure approaches in the prediction of temperatures prior and post of the shock region. This may be expected due to the region being of low turbulence, and inviscid in nature. Temperatures are also comparable in magnitude at the stationary shock front, although the prediction of its location differs between the turbulence closures. The second-moment model predicts the Mach disk location to be slightly closer to the release plane, which conforms with a slightly reduced level of mixing when compared to the two-equation model. This conforms to the observations made of the predictions of the air jet described in Section 2.1.

5. Conclusions

Presented are predictions obtained from the application of both a compressibility-corrected k-ε and a Reynolds stress transport model, to the modelling of the near-field of three previously un-reported, CO_2 jet releases. Both models are seen to perform well both qualitatively and quantitatively in the representation of the observed physics and the measured temperature field. It can be said that the performance of the two models is

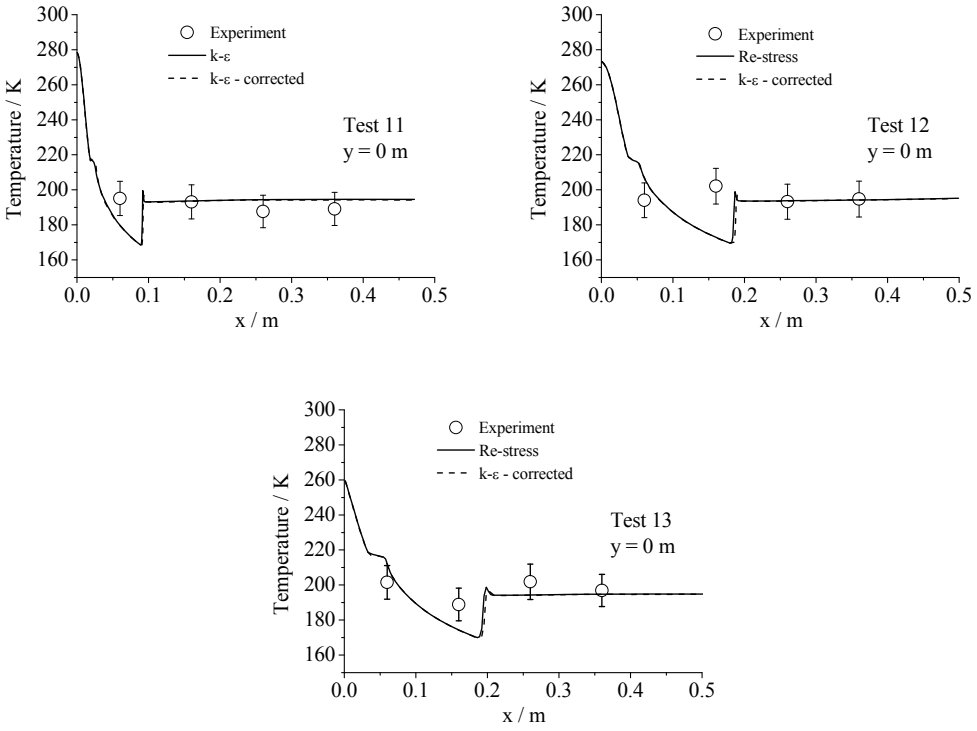

Figure 3: Centreline axial prediction of temperature in INERIS test cases, undertaken using the Re-stress and corrected k-ε models.

comparable, and discrepancy is only observed in the prediction of the location of the stationary shock front. Although it is difficult to locate the precise position of the Mach disc from the data, the second-moment model can be said to marginally conform more to these data due to its improved ability in predicting the effects of compressibility upon the turbulence dissipation. It is concluded that the nature of the second-moment closure is such that for the flows being investigated, it can be applied unmodified, with a similar level of success as a modified k-ε model within the near-field. Further investigation is currently being undertaken with respect to the models' performance in other jet regions.

6. Acknowledgements

The research leading to the results contained in this paper received funding from the European Union 7th Framework Programme FP7-ENERGY-2009-1 under grant agreement number 241346. The paper reflects only the authors' views and the European Union is not liable for any use that may be made of the information contained therein.

References

CO2PipeHaz, 2009, Quantitative Failure Consequence Hazard Assessment for Next Generation CO_2 Pipelines: The Missing Link, CO2PipeHaz Project Website, <http://www.co2pipehaz.eu/> accessed on 03/12/13.

M. Dianat, M. Fairweather, W.P. Jones, 1996, Reynolds Stress Closure Applied to Axisymmetric Impinging Turbulent Jets, Theor. Comp. Fluid. Dyn., 8, 6, 435-447.

Imperial College London, 2013, DIPPR 801 Database, <http://www.aiche.org/dippr/> accessed on 12/09/13.

C.M. Dixon, S.E. Gant, C. Obiorah, M. Bilio, 2012, Validation of Dispersion Models for High Pressure Carbon Dioxide Releases, IChemE Hazards XXIII, IChemE, Southport, UK, 153-163.

C.D. Donaldson, R.S. Snedeker, 1971, A Study of Free Jet Impingement. Part 1. Mean Properties of Free and Impinging Jets, J. Fluid Mech., 45, 2, 281-319.

M. Fairweather, K.R. Ranson, 2006, Prediction of Underexpanded Jets Using Compressibility-Corrected, Two-Equation Turbulence Models, Prog. Comput. Fluid Dy., 6, 1-3, 122-128.

N. Herzog, C. Egbers, 2013, Atmospheric dispersion of CO_2 released from pipeline leakages, Energy Procedia, 40, 232-239.

W.P. Jones, B.E. Launder, 1972, The Prediction of Laminarization with a Two-Equation Model of Turbulence, Int. J. Heat Mass Tran., 15, 2, 301-314.

W.P. Jones, P. Musonge, 1988, Closure of the Reynolds Stress and Scalar Flux Equations, Phys. Fluids, 31, 12, 3589-3604.

D.-Y. Peng, D.B. Robinson, 1976, A New Two-Constant Equation of State, Ind. Eng. Chem. Fun., 15, 1, 59-64.

S. Sarkar, G. Erlebacher, M.Y. Hussaini, H.O. Kreiss, 1991, The Analysis and Modelling of Dilatational Terms in Compressible Turbulence, J. Fluid Mech., 227, 1, 473-493.

R. Span, W. Wagner, 1996, A New Equation of State for Carbon Dioxide Covering the Fluid Region from the Triple-Point Temperature to 1100 K at Pressures up to 800 MPa, J. Phys. Chem. Ref. Data, 25, 6, 1509-1596.

C.J. Wareing, R.M. Woolley, M. Fairweather, S.A.E.G. Falle, 2013, A Composite Equation of State for the Modelling of Sonic Carbon Dioxide Jets, AIChE J., 59, 10, 3928-3942.

H.W.M. Witlox, M. Harper, A. Oke, J. Stene, 2013, Phast Validation of Discharge and Atmospheric Dispersion for Pressurised Carbon Dioxide Releases, J. Loss Prevent. Proc. 10.1016/j.jlp.2013.10.006.

R.M. Woolley, M. Fairweather, C.J. Wareing, S.A.E.G. Falle, C. Proust, J. Hebrard, D. Jamois, 2013, Experimental Measurement and Reynolds-Averaged Navier-Stokes Modelling of the Near-Field Structure of Multi-phase CO_2 Jet Releases, Int. J. Greenh. Gas Con., 18, 1, 139-149.